Published in final edited form as:
Macromolecules. 2007 ; 40(13): 4509–4515. doi:10.1021/ma0628937.

COMPLEX AMPHIPHILIC HYPERBRANCHED FLUOROPOLYMERS BY ATOM TRANSFER RADICAL SELF-CONDENSING VINYL (CO)POLYMERIZATION

Kenya T. Powell, **Chong Cheng**, and **Karen L. Wooley***
Center for Materials Innovation, Department of Chemistry and Department of Radiology, Washington University, Saint Louis, Missouri 63130-4899

Abstract

Amphiphilic hyperbranched fluorohomopolymer (M_n = 9.06 kDa, M_w/M_n= 1.90) and fluorocopolymer (M_n = 17.2 kDa, M_w/M_n= 2.50) with tri(ethylene glycol) units incorporated at the molecular level were synthesized by atom transfer radical self-condensing vinyl homopolymerization of an inimer, 4-[oxy(tri(ethylene glycol))bromoisobutyryl]-2,3,5,6-tetrafluorostyrene, and copolymerization of the inimer with 2,3,4,5,6-pentafluorostyrene (1:3, inimer:monomer), using 2,2'-bipyridine together with CuCl/$CuCl_2$ as the ligand/catalyst/deactivator system. The structure and composition of the fluoropolymers were characterized by ^{1}H, ^{13}C, and ^{19}F NMR spectroscopies. As detected by thermogravimetric analyses, the homopolymer and the copolymer had thermal stability up to 175 °C and 210 °C, respectively. Differential scanning calorimetry revealed a glass transition temperature of −19 °C for the homopolymer and 20 °C for the copolymer. Solubility tests indicated that both polymers were soluble in a broad range of organic solvents, and the presence of tri(ethylene glycol) units resulted in the formation of water dispersible micelles from each of the polymers.

Keywords

Hyperbranched; fluoropolymer; amphiphilic; oligo(ethylene glycol); atom transfer radical polymerization

INTRODUCTION

Investigations of the theory, design, preparation, and applications of highly-branched macromolecules, including dendrimers [1–12] and hyperbranched polymers (HBPs),[13–23] have been widespread over the past two decades, due to the special architectures and properties of these polymers relative to linear polymers.[24–28] HBPs are highly-branched polymers with lower structural regularity than dendrimers. Although many types of HBPs have been prepared by various synthetic pathways, polycondensation of AB_x monomers ($x \geq 2$) has remained as the traditional and most common methodology for the preparation of HBPs.[20,29]

In 1995, Fréchet *et al.* reported self-condensing vinyl polymerization (SCVP) of bifunctional *AB**monomers, called inimers.[30,31] Inimers were so named because they possessed both a monomer group (*A*) and an initiator functionality (*B**). These seminal studies led to a new approach in the production of HBPs. Although only a handful of suitable inimers were used

Corresponding author: Karen L. Wooley, Tel. (314) 935-7136, Fax (314) 935-9844, E-mail: klwooley@artsci.wustl.edu.

in early studies,[32] this methodology has been extended by constituting charge transfer complexes (CTCs) as new inimers or by copolymerization of inimers with comonomers. In 2003, Wang *et al*. reported a copolymerization of *p*-chloromethylstyrene (CMS) and chlorotrifluoroethylene (CTFE) following atom transfer radical-SCVP (ATR-SCVP) mechanism, to give a fluorinated HBP with controlled structures.[33] The electron-rich CMS was believed to assemble with electron-deficient CTFE to form a CTC that served as an inimer for the SCVP system. Self-condensing vinyl copolymerization (SCVCP) of *AB**inimers with comonomers has also significantly expanded the synthetic methodologies for the preparation of HBPs, and has provided a broad range of HBPs with diverse composition.[16,34–36] HBPs by SCVCP possess stable -*C*-*C*-backbones and have structural units that can be derived from commercially-available monomers. Their structural features, such as degrees of branching (DBs), can be controlled through the structures of the comonomer(s) and inimer(s), their feed ratios, and the copolymerization conditions.

We have a long-standing interest in hyperbranched fluoropolymers (HBFPs),[37] based upon their unique properties, including low coefficient of friction, low surface energy, low viscosity, enhanced solubility, and their facile production as compared with the production of their linear fluoropolymer counterparts.[38] Initially, our studies involved the design, synthesis, characterization, and applications of our first type hyperbranched fluoropolymer, HBFP$^{(I)}$, prepared by the polycondensation of a bis-pentafluorobenzyl ether of 3,5-dihydroxybenzyl alcohol in the presence of elemental sodium.[37,39,40] HBFP$^{(I)}$ had perfluoroaromatic rings and ether linkages throughout its structure, with pentafluorobenzyl chain-ends that can undergo nucleophilic aromatic substitution reactions for post-modification and derivatization. Furthermore, amphiphilic crosslinked networks were prepared from HBFP$^{(I)}$ and diamine-terminated poly(ethylene glycol) (DA-PEG), and their surface characteristics could be mediated by the mass ratio of HBFP to DA-PEG.[40,41] The amphiphilic crosslinked networks possessed enhanced anti-biofouling ability,[42] unusual sequestration and release behavior for a variety of small molecule guests,[43] as well as atypical mechanical performance.[44] We also recently reported the synthesis of our second type hyperbranched fluorocopolymer material, HBFP$^{(II)}$, by the ATR-SCVCP of inimer CMS with 2,3,4,5,6-pentafluorostyrene (PFS).[34] In contrast to HBFP$^{(I)}$ obtained by multi-step reactions under severe reaction conditions, HBFP$^{(II)}$ were prepared by a one-pot synthesis using commercially-available reactants under mild reaction conditions. The ATR-SCVCP method also allowed for ready control of fluorocarbon content, molecular weights, and DBs for the resulting HBFP$^{(II)}$. Moreover, HBFP$^{(II)}$-DA-PEG amphiphilic crosslinked networks were synthesized economically, and their surfaces possessed tunable structural features, with topographical-, morphological-, and compositional-heterogeneities similar to the surfaces of HBFP$^{(I)}$-DA-PEG.[45] As a result of the thermodynamically-driven phase segregation of the hydrophobic HBFP and hydrophilic PEG segments, the three-fold complexity (topography, morphology and composition) is hypothesized to be responsible for the significant anti-fouling behavior of the amphiphilic crosslinked networks. Because we hypothesized that the small size of the heterogeneities is also an important factor to enhance the resistance of protein adsorption and marine organism adhesion, we have a keen interest in the synthesis of amphiphilic structures with smaller surface domain sizes.

In our current efforts to develop new types of hyperbranched fluorocopolymer materials, our goals are to improve the anti-fouling characteristics by increasing the PEG content while retaining nanoscale surface heterogeneities. However, increasingly larger surface domain sizes were observed in crosslinked networks of HBFP$^{(II)}$-PEG with mass fractions of PEG greater than 50%. These findings necessitated the creation of a HBFP with improved PEG compatibility. Additionally, the successful production of HBFP$^{(II)}$ by ATR-SCVCP indicates that more types of hyperbranched fluoropolymers might be prepared using the same synthetic methodology. With these concepts in mind, we have developed our third type hyperbranched

fluoropolymers, HBFP$^{(III)}$ by ATRR-SCVP or SCVCP using a tri(ethylene glycol)-functionalized amphiphilic fluorinated inimer.

RESULTS AND DISCUSSION

Syntheses

In order to synthesize hyperbranched fluoropolymers **1** and **2**, having oligo(ethylene glycol) (OEG) chains incorporated within their frameworks *via* the ATR-SCVCP methodology, an OEG-functionalized fluorinated inimer **3** that possesses a polymerizable vinylic group and an initiator functionality for ATRP was prepared (Scheme 1). The formulation of such a molecule began with the nucleophilic aromatic substitution of 2,3,4,5,6-pentafluorostyrene (PFS) by tri (ethylene glycol) (TEG). In the presence of NaH in THF heated at reflux for 1.5 h, the reaction of PFS with 7.5 equiv. of TEG afforded **4** in 88% yield, after chromatographic purification. Both PFS and TEG were selected based on their commercial-availability and laboratory convenience, in addition to their well-characterized and well-understood properties. Relative to PFS, an excess of TEG was required in the preparation of **4** to suppress the side product in which both of the hydroxyl groups of TEG were arylated by PFS. Additionally, TEG, instead of longer EG segments, was chosen to maintain simplicity. Transformation of **4** into the inimer, **3**, was accomplished by allowing **4** to undergo reaction with 2-bromoisobutyryl bromide in THF at room temperature for 20 h, to give **3** in 88 % yield, after chromatographic purification.

Homopolymerization of **3** was performed using CuCl/$CuCl_2$/bipyridine as the catalyst/deactivator/ligand system ($[\mathbf{3}]_0/[CuCl]_0/[CuCl_2]_0/[bipyridine]_0$ = 1.0/0.1/0.01/0.22) in fluorobenzene (PhF) at 60 °C, and the polymerization process was monitored by ^{1}H NMR spectroscopy. As measured by ^{1}H NMR spectroscopy, comparison of the vinylic proton resonances at 5.62, 6.02 and 6.62 ppm with the proton resonances of methylene units on the α-positions to the ester oxygen and the phenyl ether group at 4.20–4.35 ppm, it was found that these reaction conditions gave a 70% conversion of the vinylic groups at 10 h, an 80% conversion at 20 h. Conversions of the alkyl halide initiating site were also observed based on the decreased resonance intensities of the methyl protons of the alkyl halide initiating site of **3** resonating at 2.05 ppm in comparison to the TEG proton signals, giving 40 and 49% conversions at 10 and 20 h, respectively. The polymerization was quenched at 24 h, and the polymerization mixture was diluted with THF and passed through an alumina column. Concentration of the solution and repeated precipitations into hexanes then gave hyperbranched fluorohomopolymer **1** in 64% yield (80 % yield based upon an estimated 80 % conversion of **3**). As determined by size exclusion chromatography (SEC) equipped with both a differential refractometer and a dynamic light scattering detector, **1** had an absolute M_n of 9.06 kDa with an M_w/M_n value of 1.90 (Figure 1a).

Copolymerization of **3** with PFS was performed to produce an amphiphilic hyperbranched fluorocopolymer that has structure somewhat similar to HBFP $^{(II)}$,[34] but possesses TEG units that were absent from HBFP$^{(II)}$. The feed ratio of PFS to **3** was 3:1 to dramatically alter the composition and structure relative to the homopolymer **1**. This ratio was also selected to mimic the feed ratio of $[monomer]_0$:$[inimer]_0$ of 3:1, which resulted in the highest fluorocarbon content for HBFP$^{(II)}$, and for later comparisons of DA-PEG crosslinked networks and copolymer **2** with HBFP$^{(II)}$-DA-PEG crosslinked networks.[45] The reaction was conducted with the initial feed ratios of $[PFS]_0/[\mathbf{3}]_0/[CuCl]_0/[CuCl_2]_0/[bipyridine]_0$ of 3.0/1.0/0.1/0.01/0.22, in PhF at 60 °C. The copolymerization process was monitored by ^{1}H NMR spectroscopy. Because of structural similarity, **3** and PFS have similar positions for the ^{1}H NMR resonances of their vinylic protons. Based upon quantitative ^{19}F NMR analysis (*vide infra*), it was determined that the structural units of **3** and PFS were present in the final copolymer **2** in a ratio equivalent to that of the original feed. Thus, **3** and PFS possessed similar reactivity under the copolymerization conditions and their percent conversions were equal to

the total percent conversion of all vinyl groups. As detected by ^{1}H NMR analysis, the conversion of the vinylic groups was 65% at 8 h and 75% at 23 h. The copolymerization was quenched at 24 h, and the copolymerization mixture was diluted with THF and passed through an alumina column. Concentration of the solution and repeated precipitations into hexanes then gave hyperbranched fluorocopolymer **2** in 56% yield (75% yield based upon 75% conversion of PFS and **3**). As determined by SEC (Figure 2b), hyperbranched fluorocopolymer **2** had an absolute M_n of 17.2 kDa with a M_w/M_n value of 2.50 (Figure 1b). As illustrated by the SEC traces of Figure 1, relative to homopolymerization of **3**, copolymerization of **3** with PFS actually gave polymers with higher molecular weights in a shorter polymerization time, presumably due to the higher polymerizable group-to-initiator site ratio for the copolymerization system.

NMR Spectroscopic Characterization

Both hyperbranched fluorohomopolymer **1** and fluorocopolymer **2** were characterized by ^{1}H, ^{13}C, and ^{19}F NMR spectroscopies. As shown in Figure 2a and 2b, both of the polymers had similar ^{1}H NMR spectra. Their backbone methylene and methine protons, resulting from the conversion of vinylic groups, resonated at 1.5–3.1 ppm as broad resonances. Relative to homopolymer **1** with only backbone protons from **3**, copolymer **2** exhibited stronger ^{1}H NMR resonances in this region because it possessed backbone protons from both **3** and PFS units. Before initiation, the methyl protons of the residual α-bromoisobutyrate groups from **3** resonated at 1.9 ppm as a sharp singlet; after initiation, the methyl protons resonated at 0.7–1.5 ppm as broad signals. The methylene protons (C***H***$_2$O) of the TEG segment from **3** resonated at 3.2– 4.5 ppm. Benzylic protons of the terminal benzylic chloride and benzylic bromide functionalities, which were formed by initiation from **3** with or without halogen exchange, resonated at 4.6–5.4 ppm as several broad peaks. Finally, the vinylic protons of the head groups, which resulted from units of **3** whose vinylic group was not polymerized, resonated at 5.6, 6.0, and 6.6 ppm.

The ^{13}C NMR spectra for hyperbranched fluorohomopolymer **1** and fluorocopolymer **2** are shown in Figure 4a and 4b, respectively. For both of the polymers, their carbons resonated in four primary regions. For the region from 20–63 ppm, the ^{13}C NMR resonances are from all backbone carbons, methyl carbons, and all halogenated aliphatic carbons. The methylene carbons (***C***H$_2$O) of the TEG segments were observed from 63–75 ppm, and the aromatic and vinylic carbons resonated over 120–149 ppm. The ^{13}C NMR resonances from 171–181 ppm were assigned to the ester carbons of the isobutyrate groups. Homopolymer **1** exhibited strong ^{13}C NMR resonances at 31.0, 55.7 and 171.5 ppm for the methyl carbons, bromide carbons, and ester carbons of the residual α-bromoisobutyrate groups from inimer **3**, which indicated that **1** contained a significant portion of repeat units that had undergone vinylic group reaction for incorporation into the polymer, but retained their non-initiated α-bromoisobutyrate groups. In the ^{13}C NMR spectrum of copolymer **2**, resonances at 171.5 ppm for the ester carbons of the residual α-bromoisobutyrate groups from inimer **3** without initiation were much weaker than the resonances at 176.6 ppm for the ester carbons of extended chains, indicating that copolymer **2** had only an insignificant amount of remaining α-bromoisobutyrate groups.

The ^{19}F NMR spectra for hyperbranched fluorohomopolymer **1** and fluorocopolymer **2** are shown in Figure 4. The *meta*-fluorines and the *ortho*-fluorines of **1** exhibited resonances concentrated at −157.1 ppm and −144.6 ppm, respectively (Figure 4a). The ratio of ^{19}F NMR resonance intensities from these two peaks were in excellent agreement with the expected fluorine number ratio of 2:2. In the ^{19}F NMR spectrum of **2** (Figure 4b), the *meta*-fluorines of the PFS units of **2** showed resonances concentrated at −161.1 ppm. Resonances of the *para*-fluorines of its PFS units and the *meta*-fluorines of its inimer **3** units overlap around 156.6 ppm. Resonances of the *ortho*-fluorines of its PFS and **3** units were observed at −143.0 ppm.

Integrations of the ^{19}F NMR resonance intensities from these three regions gave a ratio of 6:5:8, indicating a 3:1 molar ratio of PFS units to units derived from inimer **3**, which was equal to the initial molar feed ratio of PFS to **3** in this copolymerization. The results also suggested that PFS and **3** had similar reactivities under the copolymerization conditions.

Elemental Analysis

Hyperbranched fluorohomopolymer **1** and fluorocopolymer **2** were also characterized by elemental analysis. For both polymers, experimental elemental percentages of C, H, and F were close to the theoretical values, and such agreement for **2** also confirmed its composition of 3:1 molar ratio of PFS units to inimer **3** units. However, for both polymers, experimental elemental percentages of Br (9.85% for **1**; 4.22% for **2**) were significantly lower than the theoretical values (16.90% for **1**; 7.57% for **2**). Biradical coupling was considered as the major reason for the lower-than-expected bromine percentages in the polymers. Furthermore, because CuCl and $CuCl_2$ were used as catalyst/deactivator for their synthetic systems, the occurrences of halogen exchange during polymerizations were also confirmed by the presences of 0.58% of Cl in **1** and 0.78% of Cl in **2**, as detected by element analysis.

Thermal Analysis

Thermogravimetric analyses were conducted to evaluate the thermal stabilities of hyperbranched fluorohomopolymer **1** and fluorocopolymer **2** (Figure 5). Homopolymer **1** showed an early mass loss at *ca*. 100 °C, which was most likely due to water evaporation, an indication of the homopolymer's affinity for water swelling. For copolymer **2**, no thermal transition for water was observed, which suggests a diminished capacity for water-swelling, with the presence of a high molar fraction of hydrophobic PFS units. Homopolymer **1** exhibited an initial decomposition onset temperature (T_d) at 175 °C, followed by three distinct thermal decomposition ranges with midpoints at 260, 302, and 385 °C (Figure 5a). Interestingly, copolymer sample **2** (Figure 5b, solid) showed a less heterogeneous thermolytic profile with an initial T_d onset at 210 °C, indicative of greater thermal stability, and only two major thermal transitions with midpoints at 310 and 413 °C (Figure 5b, dashed). The transition from 175 to 275 °C in homopolymer **1** accounted for 10 mass % loss, and was attributed to thermal degradation of terminal halide functionalities. The reduction of the intensity of this transition in copolymer **2** was expected due to the relative decrease in terminal halides with the incorporation of PFS units. Each of these results was in good agreement with the data from elemental analyses. The percentages of mass loss for the second and third transitions of **1**, from 275 to 340 and from 340 to 425 °C were 25% and 48%, respectively. The two major thermal transitions of copolymer **2** ranged from 210 to 345 °C with a mass loss of 22 %, and from 345 to 425 °C with a mass loss of 56 %.

Differential scanning calorimetry (DSC) experiments were performed to evaluate the possible glass transition temperatures (T_g) and melting transition temperatures (T_m) of **1** and **2** (Figure 6). Homopolymer **1** displayed a low T_g at −19 °C, presumably due to its high OEG content (Figure 6a). With a high fraction of PFS units, sample **2** exhibited a T_g at 20 °C, significantly higher than that of sample **1**. However, this value is much lower than that observed at 110 °C for the HBFP$^{(II)}$ copolymer based upon PFS and CMS. Additionally, no melting endotherm was observed for **1** or **2** on heating up to 150 °C (not shown), a sign of the absence of PEG domains within the polymer materials, in contrast to the amphiphilic networks of HBFP$^{(II)}$ and DA-PEG that allowed for phase segregation and crystallization of the PEG component, giving a T_m onset at 30 °C.[45]

Solubility

Similar to that observed for HBFP$^{(II)}$, solubility studies of hyperbranched fluorohomopolymer **1** and fluorocopolymer **2** were performed at room temperature, and it was found that **1** and **2**

were soluble in a broad range of organic solvents, including tetrahydrofuran, chloroform, methylene chloride, benzene, toluene, and acetone. Non-solvents based upon direct precipitation for these polymers were hexanes, methanol, and water. Thus, the incorporation of TEG did not result in a significant improvement in the water solubility of either **1** or **2**, although both polymers showed evidence of water swelling. We attribute these results to the significant hydrophobic compositions in **1** and **2**. However, the presence of TEG did modify the characteristics of the polymers. For instance, upon the slow addition of nanopure water to a dilute solution of **1** or **2** in THF (10 mg/mL), followed by dialysis of the THF against distilled water, water dispersible micelles were formed. As detected by dynamic light scattering (DLS) measurements, the micelles of **1** had a number-average hydrodynamic diameter ($D_{h,n}$) of 170 ± 20 nm and a volume-average hydrodynamic diameter ($D_{h,v}$) of 190 ± 10 nm, and the micelles of **2** had a $D_{h,n}$ of 210 ± 20 nm and a $D_{h,v}$ of 240 ± 20 nm. These encouraging results suggest that hyperbranched fluorocopolymers produced with inimers containing longer EG chains may display appreciably greater water solubility. Further evaluation of the aqueous solution-based assembly of these polymers, **1** and **2**, and others having greater OEG content are underway and will be reported elsewhere.

CONCLUSIONS

Amphiphilic hyperbranched fluorohomopolymer and fluorocopolymer have been prepared by ATR-SCVP of an amphiphilic fluorinated inimer and SCVCP of the inimer with a comonomer. The presence of covalently-attached TEG units was found to have a significant effect on the observed spectroscopic, thermal, and solution-state properties of the polymers. NMR spectroscopic characterization confirmed the structure and composition of both polymers, while thermal analyses revealed a decrease in thermal stability for **1**, but a similar thermal degradation profile for **2** relative to HBFP$^{(II)}$. Both **1** and **2** displayed a single glass transition temperature, each having a T_g value that was lower than that expected for a styrenyl-based backbone, which was an indication of well-incorporated TEG units. Moreover, the T_g for **1** was lower than that of **2**, due in part to a lower molecular weight value, as well as an increased TEG content. Polymers **1** and **2** were both soluble in a broad range of organic solvents. Neither polymer possessed appreciable water solubility, however, they underwent aggregation to afford nanoscale, intermolecular, complex micelles.. The formation of **1** and **2** with increasingly larger ethylene glycol chains is currently under investigation and these materials are being developed as potential ^{19}F MRI agents. Both **1** and **2** possess secondary and tertiary bromides and chlorides as well as a tetrafluorophenyl moiety, and **2** also has pentafluorophenyl groups that contain *para*-fluorine reactive sites. The secondary and tertiary bromides and *p*-fluorines are expected to be of great importance in future studies, as they may be utilized for polymer post-modification through atom transfer radical, substitution, or nucleophilic aromatic substitution reactions. Relative to HBFP$^{(I)}$ and HBFP$^{(II)}$, HBFP$^{(III)}$ is expected to have greater miscibility with DA-PEG, to lead to decreased domain sizes for their resulting crosslinked networks. These materials are also expected to exhibit increased surface wettability and improved mechanical robustness, without the loss of fluorocarbon content, architectural advantages, three-fold complexity, or ease of production. Thus, we are also investigating the reaction of **1** and **2** with diamine-terminated poly(ethylene glycol) in the preparation of complex, amphiphilic networks for anti-biofouling applications, among others.

EXPERIMENTAL SECTION

Materials

2,3,4,5,6-Pentafluorostyrene (PFS) was distilled over CaH_2 and stored under argon at 4.0 °C. All other chemicals and reagents were purchased from Aldrich Chemical Company and used as received.

Characterization Methods

^{1}H NMR spectra were recorded at 300 MHz on solutions in $CDCl_3$ on a Varian Mercury 300 spectrometer, with the solvent proton signal as standard. ^{13}C NMR spectra were recorded at 150.8 MHz on solutions in $CDCl_3$ on a Varian Unity 600 spectrometer with the solvent carbon signal as standard. ^{19}F NMR spectra were recorded at 282.2 MHz on solutions in $CDCl_3$ on a Varian Mercury 300 spectrometer with external $CFCl_3$ as standard. IR spectra were recorded on a Perkin-Elmer Spectrum BX FT-IR system as thin films on KBr disks and were analyzed using FT-IR Spectrum v2.00 software (Perkin-Elmer Corporation, Beaconsfield, Bucks, England).

Size exclusion chromatography (SEC) was conducted on a Waters 1515 HPLC (Waters Chromatography, Inc.) equipped with a Waters 2414 differential refractometer, a PD2020 dual-angle (15° and 90°) light scattering detector (Precision Detectors, Inc.), and a three-column series PL gel 5μm Mixed C, 500 Å, and 10^4 Å, 300 × 7.5 mm columns (Polymer Laboratories, Inc.). The system was equilibrated at 35 °C in anhydrous THF, which served as the polymer solvent and eluent with a flow rate of 1.0 mL/min. Polymer solutions were prepared at a known concentration (*ca.* 3 mg/mL) and an injection volume of 200 μL was used. Data collection and analysis were performed, respectively, with Precision Acquire software and Discovery 32 software (Precision Detectors, Inc.). Interdetector delay volume and the light scattering detector calibration constant were determined by calibration using a nearly monodispersed polystyrene standard (Pressure Chemical Co., M_p = 90 kDa, M_w/M_n < 1.04). The differential refractometer was calibrated with standard polystyrene reference material (SRM 706 NIST), of known specific refractive index increment *dn/dc* (0.184 mL/g). The *dn/dc* values of the analyzed polymers were then determined from the differential refractometer response.

Thermogravimetric analysis (TGA) was performed on a TGA/SDTA851^e instrument (Mettler-Toledo, Inc.) measuring the total mass loss on approximately 5 mg samples from 25 to 550 °C at a heating rate of 10 °C/min in a nitrogen flow of 50 mL/min. Glass transition temperature (T_g) and/or melting transition temperature (T_m) determinations were measured by differential scanning calorimetry (DSC) on a DSC822^e instrument (Mettler-Toledo, Inc.) in a temperature range of −75 to 150 °C with a heating rate of 10 °C/min under nitrogen. For both TGA and DSC, data were acquired and analyzed with STAR^e software (Mettler-Toledo, Inc.). The T_g values were taken at the midpoint of the inflection tangent and T_m values were taken as the onset, upon the third heating scans.

Hydrodynamic diameters (D_z, D_n) and size distributions for the micellar aggregates in aqueous solutions were determined by dynamic light scattering (DLS). The DLS instrumentation consisted of a Brookhaven Instruments Limited (Holtsville, NY) system, 90Plus. Measurements were made at rt. Scattered light was collected at a fixed angle of 90°. Only measurements in which the measured and calculated baselines of the intensity autocorrelation function agreed to within 0.1% were used to calculate particle size. The calculations of the particle size distributions and distribution averages were performed with the ISDA software package (Brookhaven Instruments Company), which employed CONTIN analysis, and non-negatively constrained least-squares particle size distribution analysis routines.

Elemental Analysis was performed by Galbraith Laboratories, Inc., Knoxville, TN, USA.

Synthesis of 4-[oxy(tri(ethylene glycol))]-2,3,5,6-tetrafluorostyrene (4)

2,3,4,5,6-Pentafluorostyrene (1.96 g, 10.0 mmol), tri(ethylene glycol) (11.3 g, 75 mmol), and NaH (0.380 g, 15.0 mmol) were allowed to react in presence of THF (80.0 mL) at reflux for 1.5 h. The residue was partitioned between CH_2Cl_2 and saturated ammonium chloride solution. The combined organic layers were concentrated and the product was isolated by silica gel

column chromatography with hexane:CH_2Cl_2 (1:1) as eluent and increasing polarity to 3 % MeOH in CH_2Cl_2. Yield = 88%; IR: 3600-3200, 3050-2820, 1660-1620, 1530-1400, 1350, 1290, 1250, 1180-1060, 980-960, 940, 890, 860, 670 cm^{-1}; ^1H NMR ($CDCl_3$): δ 2.32 (t, J = 6.0 Hz, 1H, O***H***), 3.59 (t, J = 4.5 Hz, 2H, HOC***H***$_2$), 3.63-3.75 (m, 6H, OC***H***$_2$), 3.83 (t, J = 4.5 Hz, 2H, OC***H***$_2$), 4.38 (t, J = 4.5 Hz, 2H, OC***H***$_2$), 5.62 (d, J = 12.0 Hz, 1H, *cis* C***H***H=CHAr), 6.02 (d, J = 18.0 Hz, 1H, *trans* CH***H***=CHAr), 6.62 (dd, J = 12.0 Hz and 18.0 Hz, 1H, CH_2=C***H***Ar) ppm; ^{13}C NMR ($CDCl_3$): δ 61.9, 70.3, 70.5, 71.1, 72.6, 74.3, 111.1, 122.2, 122.3, 122.4, 122.5, 136.2, 139.6, 143.0, 143.5, 146.9 ppm; ^{19}F NMR ($CDCl_3$): δ-158.5 (m, 2F, *meta*-F), -145.5 (m, 2F, *ortho*-F) ppm; Anal. Calc'd. $C_{14}H_{16}O_4F_4$ (324.27 Da): C, 51.86; H, 4.97; F, 23.44 %. Found C, 51.28; H, 4.97; F, 22.10 %.

Synthesis of 4-[oxy(tri(ethylene glycol))bromoisobutyryl]-2,3,5,6-tetrafluorostyrene (3)

To a reaction flask containing **4** (11.8 g, 36.3 mmol), pyridine (11.5 g, 145 mmol), and THF (80.0 mL), was added 2-bromoisobutyryl bromide (25.1 g, 109 mmol) dropwise. The mixture was allowed to react at room temperature for 20 h. The residue was partitioned between CH_2Cl_2 and H_2O and the aqueous layer was extracted with CH_2Cl_2 (× 3). The organic layers were combined, dried over $MgSO_4$, filtered, and the solvent evaporated *in vacuo*. The product was isolated by silica gel column chromatography with hexane:CH_2Cl_2 (1:1) as eluent and increasing polarity to 3 % MeOH in CH_2Cl_2. Yield = 88%; IR: 3050-2820, 1750-1720, 1660-1620, 1530-1400, 1390, 1370, 1355, 1280, 1180-1060, 1030, 980-960, 940, 860, 760, 645 cm^{-1}; ^1H NMR ($CDCl_3$): δ 1.93 (s, 6H, CC***H***$_3$), 3.63-3.76 (m, 6H, OC***H***$_2$), 3.83 (t, J = 4.5 Hz, 2H, OC***H***$_2$); 4.32 (br t, J = 4.5 Hz, 2H, OC***H***$_2$); 4.37 (br t, J = 4.5 Hz, 2H, OC***H***$_2$); 5.62 (d, J = 12.0 Hz, 1H, *cis* C***H***H=CHAr), 6.02 (d, J = 18.0 Hz, 1H, *trans* CH***H***=CHAr), 6.62 (dd, J = 12.0 Hz and 18.0 Hz , 1H, CH_2=C***H***Ar) ppm; ^{13}C NMR ($CDCl_3$): δ 30.5, 55.6, 64.9, 70.1, 70.6, 74.1, 77.0, 77.3, 77.5, 110.6, 121.8, 122.0, 136.4, 140.2, 141.8, 144.0, 145.7, 171.3 ppm; ^{19}F NMR ($CDCl_3$): δ-158.7 (m, 2F, *meta*-F), -145.9 (m, 2F, *ortho*-F) ppm; Anal. Calc'd. for $C_{18}H_{21}O_5F_4Br$ (473.26 Da): C, 45.69; H, 4.47; F, 16.06; Br, 16.90 %. Found C, 44.63; H, 4.35; F, 15.56; Br, 19.07 %.

Synthesis of hyperbranched fluorohomopolymer (1)

To a reaction flask with a magnetic stirring bar, **3** (1.42 g, 1.0 eq.), BiPy (0.103 g, 0.22 eq.), CuCl (0.0296 g, 0.1 eq.), $CuCl_2$ (0.004 g, 0.01 eq.), and 18 PhF (4.0 mL, 80 vol %) were added. The reaction mixture was degassed by at least three cycles of freeze-pump-thaw, and then heated with an oil bath at 60 °C. During polymerization, small aliquots of polymerization were withdrawn with syringe, and were analyzed by ^1H NMR spectroscopy for the determination of conversion of vinylic bonds based on the remaining vinylic proton resonances at 5.62, 6.02 and 6.62 ppm. Finally, the polymerization was quenched, by being allowed to cool to rt, and then opening of the flask to air and dilution of the reaction mixture by addition of THF, at a polymerization time of 24 h, with an estimated conversion of vinylic bonds of 80%. The polymerization solution was passed through an alumina column, eluted with THF, precipitated three times into hexanes, and dried *in vacuo* to give 0.91 g of viscous, pale yellow oil. Yield = 64 %; $M_{n,SEC}$ = 9.06 kDa, M_w/M_n = 1.99; T_g = − 19 °C; TGA in N_2: 175 – 275 °C, 10 % mass loss, 275– 340 °C, 25 % mass loss, 340 – 425 °C, 48 % mass loss; IR: 3010-2850, 1745-1725, 1650, 1510-1410, 1390, 1370, 1353, 1280, 1180-1065, 1040, 980-950, 885, 765, 645 cm^{-1}; ^1H NMR ($CDCl_3$): δ 0.70–1.50 (br m, CC***H***$_3$), 1.50–3.10 (br m, aliphatic backbone protons), 1.92 (s, CC***H***$_3$), 3.20–4.40 (br m, C***H***$_2$O protons of OEG units), 4.60–5.40 (br m, ArC***H***Br and ArC***H***Cl), 5.65 (*cis* C***H***H=CHAr), 6.02 (*trans* CH***H***=CHAr), 6.60 (CH_2=C***H***Ar) ppm; ^{13}C NMR ($CDCl_3$): δ 22.9–28.3, 31.0, 35.7–47.9, 55.7, 63.1–63.8, 65.1, 68.7, 70.1–71.1, 74.2, 110.7–116.5, 122.0, 137.2, 141.0, 144.6, 171.5, 176.0–177.6, 181.1 ppm; ^{19}F NMR ($CDCl_3$): δ-157 (m, *meta*-F), -144 (m, *ortho*-F) ppm; Anal. Calc'd. for $C_{18}H_{21}O_5F_4Br$ (473.26 Da): C, 45.69; H, 4.47; F, 16.06; Br, 16.90 %. Found C, 46.80; H, 4.73; F, 15.52; Br, 9.85; Cl, 0.58%.

Synthesis of hyperbranched fluorocopolymer (2)

To a reaction flask with a magnetic stirring bar, 2,3,4,5,6-Pentafluorostyrene (1.23 g, 3.0 eq.), **3** (1.00 g, 1.0 eq.), BiPy (0.217 g, 0.66 eq.), CuCl (0.0627 g, 0.3 eq.), $CuCl_2$ (0.009 g, 0.03 eq.), and PhF (5.0 mL, 70 v%) were added. The reaction mixture was degassed by at least three cycles of freeze-pump-thaw, and then heated with an oil bath at 60 °C. During polymerization, small aliquots of polymerization were withdrawn with syringe, and were analyzed by ^{1}H NMR spectroscopy for the determination of conversion of vinylic bonds based on the remaining vinylic proton resonances at 5.62, 6.02 and 6.62 ppm. Finally, the polymerization was quenched, by being allowed to cool to rt, and then opening of the flask to air and dilution of the reaction mixture by addition of THF, at a polymerization time of 24 h, with an estimated conversion of vinylic bonds of 75%. The polymerization solution was passed through an alumina column, eluted with THF, precipitated three times into hexanes, and dried *in vacuo* to give 1.24 g of crystalline, white solid. Yield = 56%; $M_{n,\,SEC}$ = 17.2 kDa, M_w/M_n = 2.48; T_g = 20.4 °C; TGA in N_2: 210 – 345 °C, 22 % mass loss, 345 – 425 °C, 56 % mass loss; IR: 3010-2850, 1740-1720, 1650, 1540-1410, 1390, 1370, 1300, 1215, 1175-1065, 1085, 1000-930, 880, 760 cm^{-1}; ^{1}H NMR ($CDCl_3$): δ 0.70–1.50 (br m, CC***H***$_3$), 1.50–3.10 (br m, aliphatic backbone protons), 1.92 (s, CC***H***$_3$), 3.20–4.40 (br m, C***H***$_2$O protons of OEG units), 4.60–5.40 (br m, ArC***H***Br and ArC***H***Cl), 5.65 (*cis*C***H***H=CHAr), 6.02 (*trans* CH***H***=CHAr), 6.60 (CH_2=C***H***Ar) ppm; ^{13}C NMR ($CDCl_3$): δ 24.7, 29.7–30.7, 32.1–41.7, 63.6, 68.8, 70.0–70.8, 74.3, 114.7, 122.2, 137.6, 140.7, 144.7, 176.6 ppm; ^{19}F NMR ($CDCl_3$): δ-162 (m, *meta*-F (PFS)), -157 (m, *para*-F (PFS) and *meta*-F (TFS)), -143 (m, *ortho*-F (PFS and TFS) ppm; Anal. Calc'd. for $C_{42}H_{30}O_5F_{19}Br$ (3:1 PFS:**3**): C, 47.79; H, 2.86; F, 34.20; Br, 7.57 %. Found C, 48.97; H, 3.04; F, 33.06; Br, 4.22 %; Cl, 0.78 %.

ACKNOWLEDGMENTS

Financial support from the Office of Naval Research (N00014-05-1-0057) is gratefully acknowledged. This material is also based upon work supported by the National Heart Lung and Blood Institute of the National Institutes of Health as a Program of Excellence in Nanotechnology (HL080729), and the McDonnell Pediatric Cancer Center of the Children's Discovery Institute at Washington University. We also thank the Washington University Dean's Fellowship Program (KTP) and Unilever Corporation (CC) for Ph.D. student and postdoctoral fellowship support, respectively.

References

1. Tomalia DA, Fréchet JMJ. J. Polym. Sci., Part A: Polym. Chem 2002;40:2719–2728.
2. Dvornic PR. J. Polym. Sci., Part A: Polym. Chem 2006;44:2755–2773.
3. Hecht S. J. Polym. Sci., Part A: Polym. Chem 2003;41:1047–1058.
4. Steffensen MB, Hollink E, Kuschel F, Bauer M, Simanek EE. J. Polym. Sci., Part A: Polym. Chem 2006;44:3411–3433.
5. Li W-S, Kim KS, Jiang D-L, Tanaka H, Kawai T, Kwon JH, Kim D, Aida T. J. Am. Chem. Soc 2006;128:10527–10532. [PubMed: 16895420]
6. Vögtle F, Fakhrnabavi H, Lukin O. Org. Lett 2004;6:1075–1078. [PubMed: 15040726]
7. Banerjee D, Broeren MAC, van Genderen MHP, Meijer EW, Rinaldi PL. Macromolecules 2004;37:8313–8318.
8. Garcia-Martinez JC, Lezutekong R, Crooks RM. J. Am. Chem. Soc 2005;127:5097–5103. [PubMed: 15810844]
9. McCarthy TDKP, Henderson SA, Giannis M, O'Keefe DF, Heery G, Paull JRA, Matthews BR, Holan G. Molecular Pharmaceutics 2005;2:312–318. [PubMed: 16053334]
10. McGrath DV. Molecular Pharmaceutics 2005;2:253–263. [PubMed: 16053328]
11. Venditto VJ, Regino CAS, Brechbiel MW. Molecular Pharmaceutics 2005;2:302–311. [PubMed: 16053333]
12. Zhai X, Peleshanko S, Klimenko NS, Genson KL, Vaknin D, Vortman MY, Shevchenko VV, Tsukruk VV. Macromolecules 2003;36:3101–3110.

13. Froehling P. J. Polym. Sci., Part A: Polym. Chem 2004;42:3110–3115.
14. Kim YH. J. Polym. Sci., Part A: Polym. Chem 1998;36:1685–1698.
15. Kubisa P. J. Polym. Sci., Part A: Polym. Chem 2003;41:457–468.
16. Cheng K-C, Chuang T-H, Chang J-S, Guo W, Su W-F. Macromolecules 2005;38:8252–8257.
17. Gittins PJ, Twyman LJ. J. Am. Chem. Soc 2005;127:1646–1647. [PubMed: 15700992]
18. Marcos AG, Pusel TM, Thomann R, Pakula T, Okrasa L, Geppert S, Gronski W, Frey H. Macromolecules 2006;39:971–977.
19. Unal S, Long TE. Macromolecules 2006;39:2788–2793.
20. Voit B. J. Polym. Sci., Part A: Polym. Chem 2000;38:2505–2525.
21. Wu D-C, Liu Y, Jiang X, He C-B, Goh SH, Leong KW. Biomacromolecules 2006;7:1879–1883. [PubMed: 16768410]
22. Yan XZ, Goodson T III. J. Phys. Chem. B 2006;110:14667–14672. [PubMed: 16869570]
23. Zhang J, Wang H, Li X. Polymer 2006;47:1511–1518.
24. Fréchet JMJ. J. Polym. Sci., Part A: Polym. Chem 2003;41:3713–3725.
25. Hawker CJ, Chu F. Macromolecules 1996;29:4370–4380.
26. Hawker CJ, Farrington PJ, Mackay ME, Wooley KL, Frechet JMJ. J. Am. Chem. Soc 1995;117:4409–4410.
27. Wooley KL, Fréchet JMJ, Hawker CJ. Polymer 1994;35:4489–4495.
28. Wooley KL, Klug CA, Tasaki K, Schaefer J. J. Am. Chem. Soc 1997;119:53–58.
29. Voit B. J. Polym. Sci., Part A: Polym. Chem 2005;43:2679–2699.
30. Hawker CJ, Fréchet JMJ, Grubbs RB, Dao J. J. Am. Chem. Soc 1995;117:10763–10764.
31. Fréchet JMJ, Henmi M, Gitsov I, Aoshima S, Leduc MR, Grubbs RB. Science 1995;269:1080–1083. [PubMed: 17755528]
32. Weimer MW, Fréchet JMJ, Gitsov I. J. of Polym. Sci., Part A: Polym. Chem 1998;36:955–970.
33. Wang W, Yan D, Bratton D, Howdle SM, Wang Q, Lecomte P. Adv. Mater 2003;15:1348–1352.
34. Cheng C, Wooley KL, Khoshdel E. J. Poly. Sci., Part A: Poly. Chem 2005;43:4754–4770.
35. Gong F, Tang H, Liu C, Jiang B, Ren Q, Yang Y. J. Applied Polym. Sci 2006;101:850–856.
36. Hong C-Y, Zou Y-F, Pan C-Y. Polymer International 2003;52:257–264.
37. Mueller A, Kowalewski T, Wooley KL. Macromolecules 1998;31:776–786.
38. Powell KT, Cheng C, Gudipati CS, Wooley KL. J. Mater. Chem 2005;15:5128–5135.
39. Gooden JK, Gross ML, Mueller A, Stefanescu AD, Wooley KL. J. Am. Chem. Soc 1998;120:10180–10186.
40. Gan D, Mueller A, Wooley KL. J. Polym. Sci., Part A: Polym. Chem 2003;41:3531–3540.
41. Gudipati CS, Greenlief CM, Johnson JA, Prayongpan P, Wooley KL. J. Poly. Sci. Part A: Poly. Chem 2004;42:6193–6208.
42. Gudipati CS, Finlay JA, Callow JA, Callow ME, Wooley KL. Langmuir 2005;21:3044–3053. [PubMed: 15779983]
43. Brown GO, Bergquist C, Ferm P, Wooley KL. J. Am. Chem. Soc 2005;127:11238–11239. [PubMed: 16089441]
44. Xu J, Bohnsack DA, Mackay ME, Wooley KL. J. Am. Chem. Soc 2007;129:506–507. [PubMed: 17227010]
45. Powell KT, Cheng C, Wooley KL, Singh A, Urban MW. J. Polym. Sci., PartA: Polym. Chem 2006;44:4782–4794.

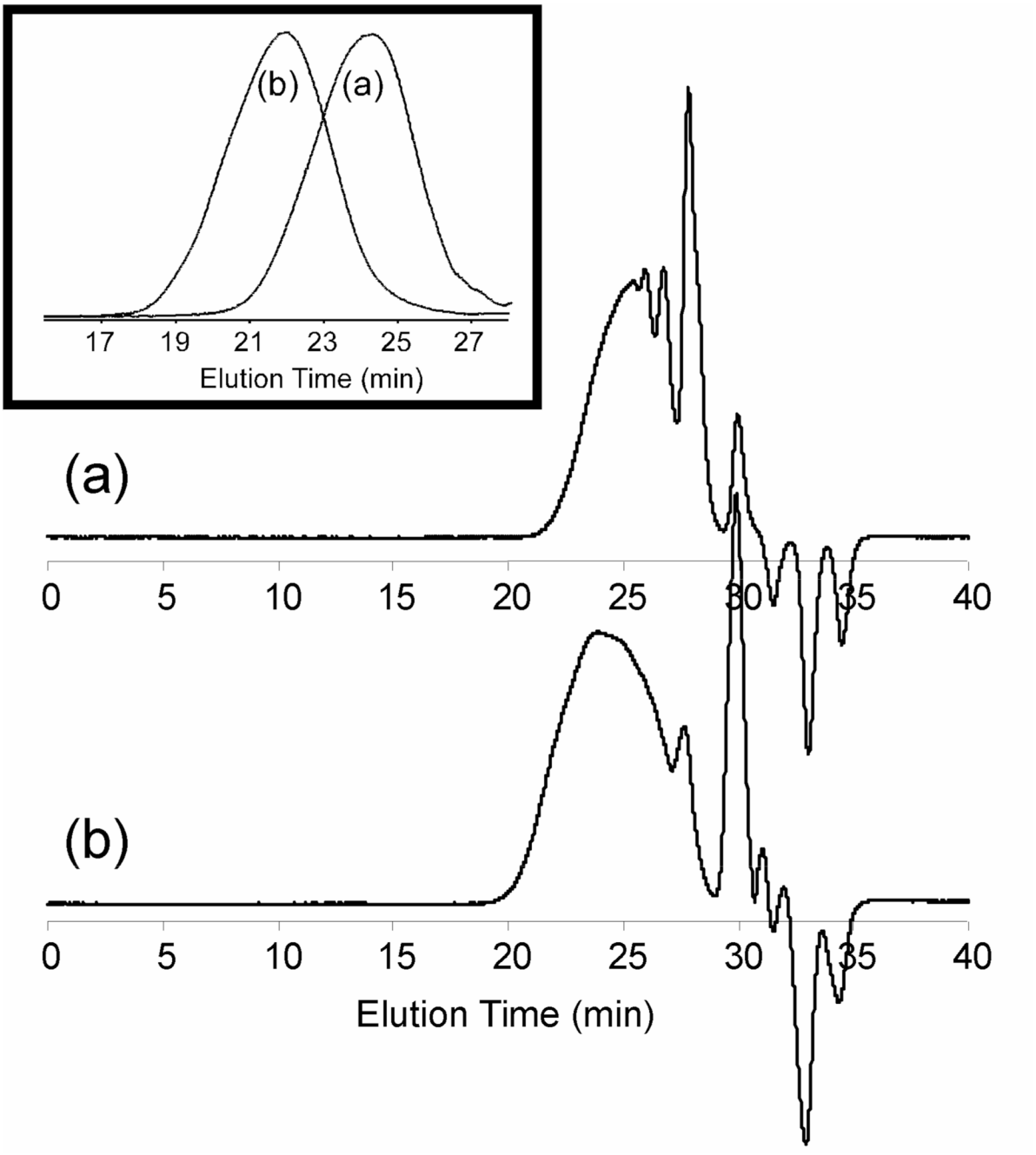

Figure 1.
SEC traces for (a) homopolymerization of **3** at t = 10 h and (b) copolymerization of **3** and PFS at t = 8 h , with SEC traces of the final purified polymers **1** and **2** (t = 24 h) included as insets.

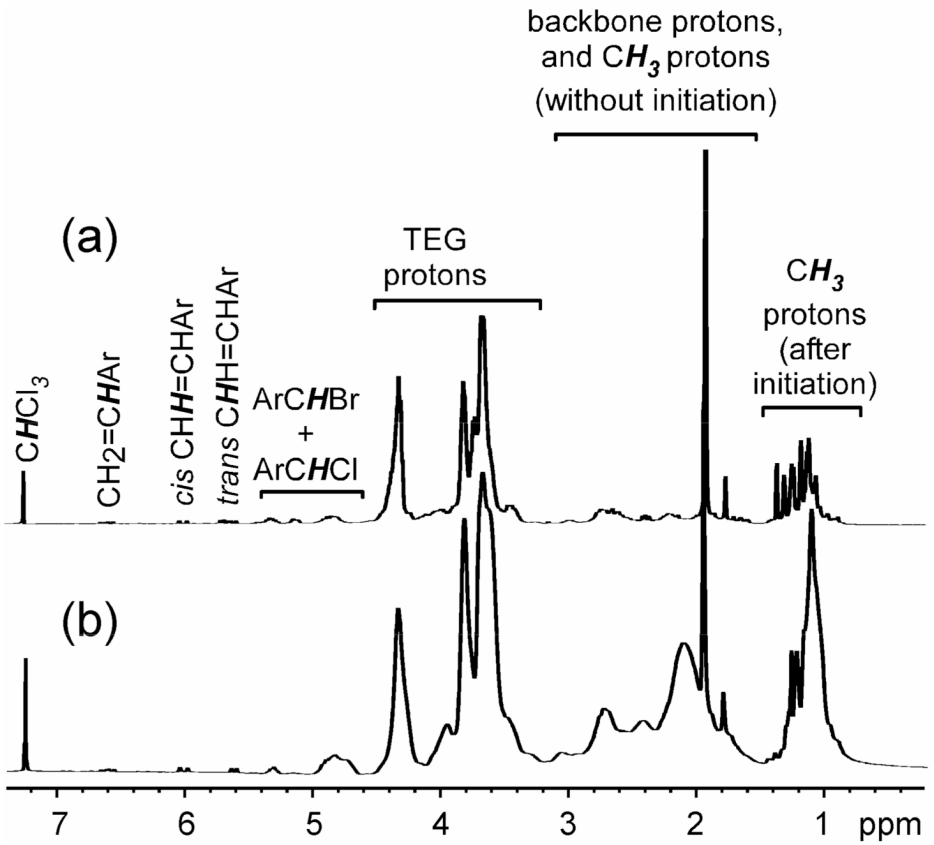

Figure 2.
^{1}H NMR (300 MHz, CDCl**3**) spectra for (a) hyperbranched fluorohomopolymer **1**, and (b) hyperbranched fluorocopolymer **2**.

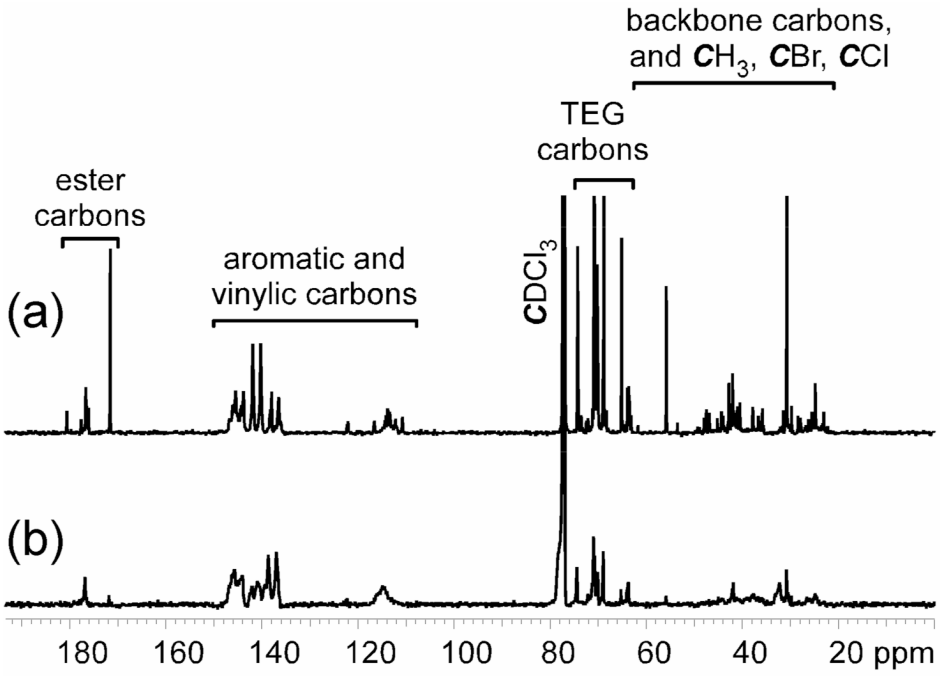

Figure 3.
^{13}C NMR (150.8 MHz, $CDCl_3$) spectra for (a) hyperbranched fluorohomopolymer **1**, and (b) hyperbranched fluorocopolymer **2**.

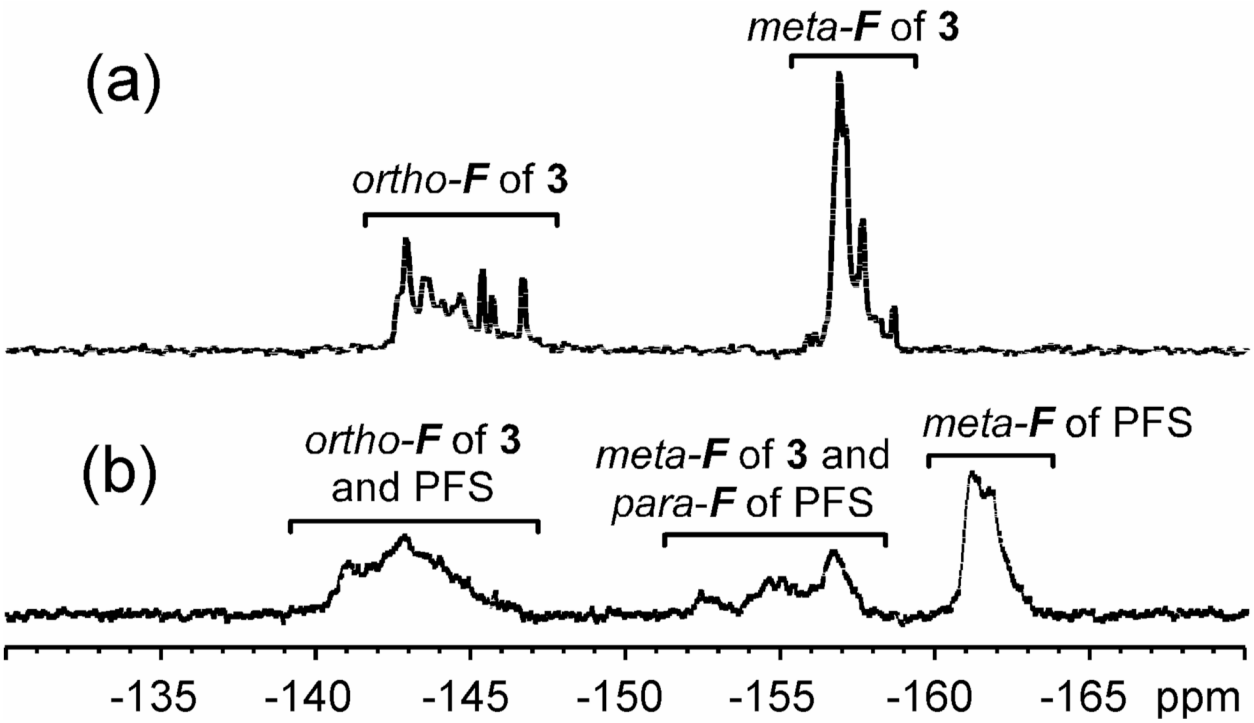

Figure 4.
^{19}F NMR (282 MHz, $CDCl_3$) spectra for (a) hyperbranched fluorohomopolymer **1** and (b) hyperbranched fluorocopolymer **2**.

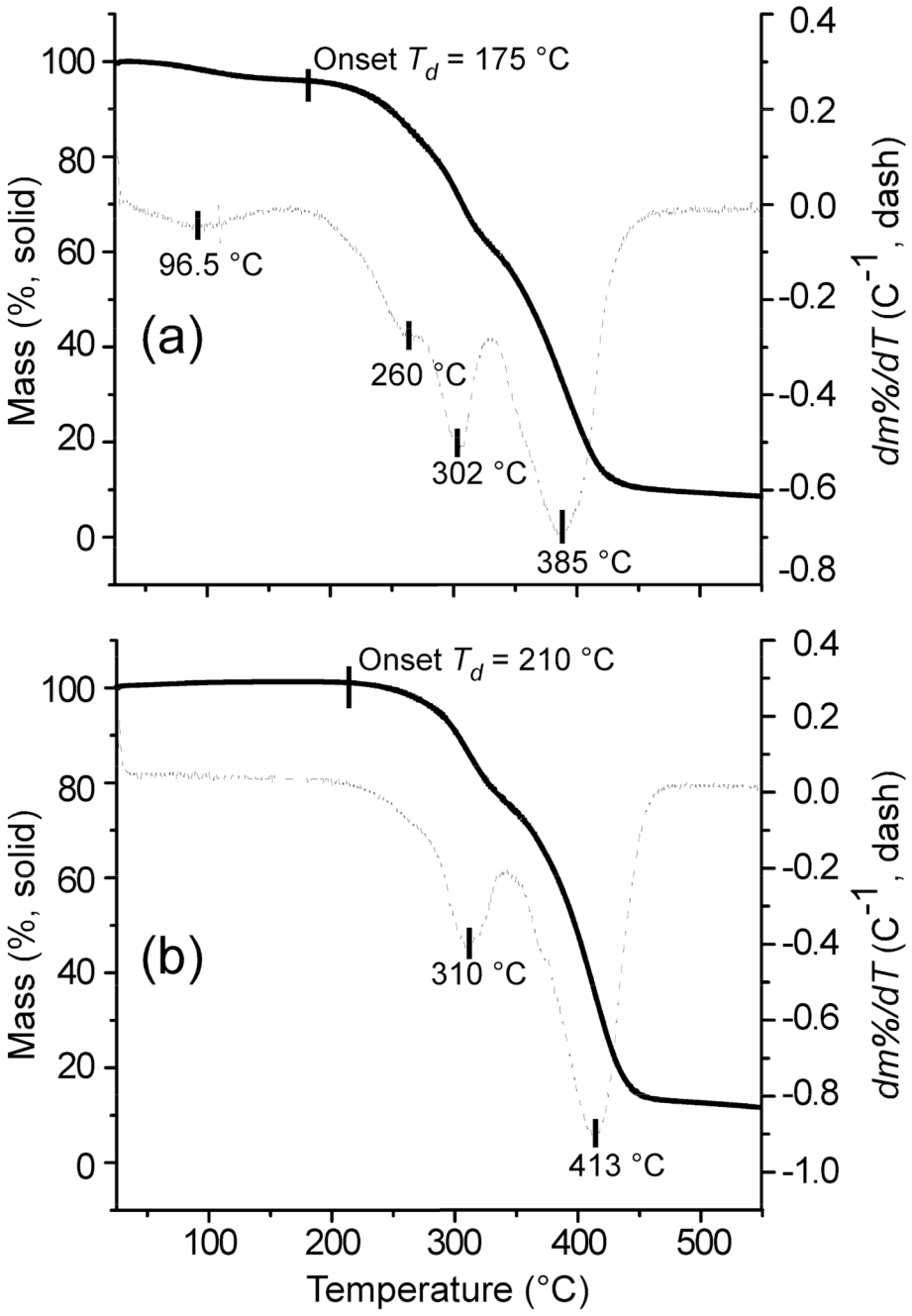

Figure 5.
Thermolytic profiles for (a) hyperbranched fluorohomopolymer **1**, and (b) hyperbranched fluorocopolymer **2**. Mass % is illustrated with solid lines and the first derivative plots are shown as dashed lines.

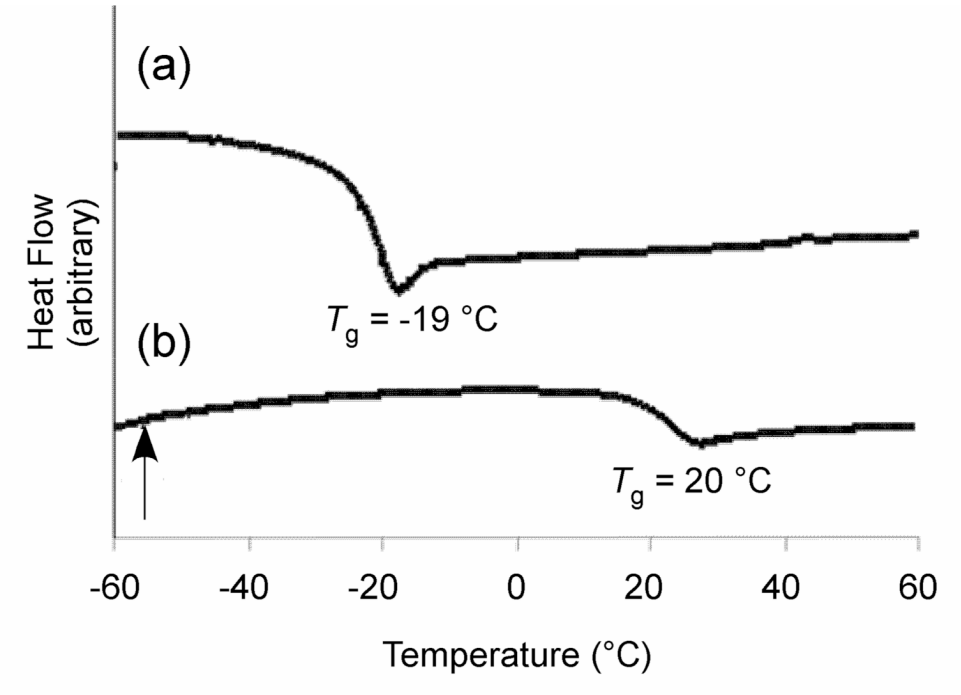

Figure 6.
DSC thermograms for (a) hyperbranched fluorohomopolymer **1**, and (b) hyperbranched fluorocopolymer **2**.

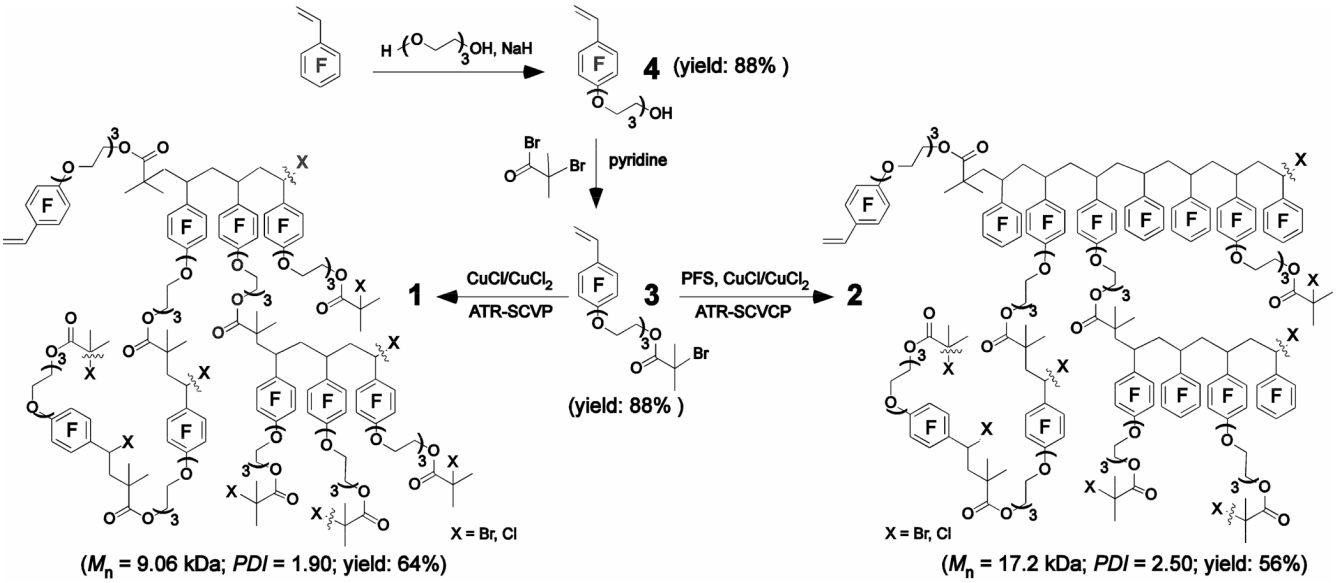

Scheme 1.

Syntheses of hyperbranched fluorohomopolymer **1** and fluorocopolymer **2** by atom transfer radical vinyl self-condensing vinyl (co)polymerization.